Insight on AV-45 binding in white and grey matter from histogram analysis: a study on early Alzheimer's disease patients and healthy subjects.

Federico Nemmi, Laure Saint-Aubert, Djilali Adel, Anne-Sophie Salabert, Jérémie Pariente, Emmanuel J. Barbeau, Pierre Payoux, Patrice Péran

Insight on AV-45 binding in white and grey matter from histogram analysis: study on early Alzheimer's disease and healthy subjects

Federico Nemmi*[a,b], Laure Saint-Aubert*[a,b], Djilali Adel[a,b,c], Anne-Sophie Salabert[a,b,c], Jérémie Pariente[a,b,d], Emmanuel J. Barbeau[d,e], Pierre Payoux[a,b,c] and Patrice Péran[a,b]

[a] Inserm, imagerie cérébrale et handicaps neurologiques UMR 825, Centre Hospitalier Universitaire de Toulouse, Toulouse, France ;

[b] Université de Toulouse, UPS, imagerie cérébrale et handicaps neurologiques UMR 825, Centre Hospitalier Universitaire de Toulouse, Toulouse, France ;

[c] Service de Médecine Nucléaire, Pôle Imagerie, Centre Hospitalier Universitaire de Toulouse, Toulouse, France ; [d] Service de neurologie, pôle neurosciences, Centre Hospitalier Universitaire de Toulouse, Toulouse, France ;

[e] Université de Toulouse, UPS, centre de recherche cerveau et cognition, France, CNRS, CerCo, Toulouse, France

* These authors contributed equally to this work

First and corresponding Author: Federico Nemmi, Ph.D.

Place du Dr. Baylac, CHU Purpan, Pavillon Baudot

31059, Toulouse cedex 9, France.

federico.nemmi@gmail.com

Tel :0033562746194

Fax :0033562746163

Abstract

Purpose: AV-45 amyloid biomarker is known to show uptake in white matter in patients with Alzheimer's disease (AD) but also in healthy population. This binding; thought to be of a non-specific lipophilic nature has not yet been investigated. The aim of this study was to determine the differential pattern of AV-45 binding in healthy and pathological populations in white matter.

Methods: We recruited 24 patients presenting with AD at early stage and 17 matched, healthy subjects. We used an optimized PET-MRI registration method and an approach based on intensity histogram using several indexes. We compared the results of the intensity histogram analyses with a more canonical approach based on target-to-cerebellum Standard Uptake Value (SUVr) in white and grey matters using MANOVA and discriminant analyses. A cluster analysis on white and grey matter histograms was also performed.

Results: White matter histogram analysis revealed significant differences between AD and healthy subjects, which were not revealed by SUVr analysis. However, white matter histograms was not decisive to discriminate groups, and indexes based on grey matter only showed better discriminative power than SUVr. The cluster analysis divided our sample in two clusters, showing different uptakes in grey but also in white matter.

Conclusion: These results demonstrate that AV-45 binding in white matter conveys subtle information not detectable using SUVr approach. Although it is not better than standard SUVr to discriminate AD patients from healthy subjects, this information could reveal white matter modifications.

Keywords: AV-45, amyloid, intensity histogram, discrimination analysis, Alzheimer's disease

1. Introduction

Florbetapir (AV-45) radioligand has been shown to bind amyloid peptide with good affinity [1, 2]. Correlations between AV-45 uptake and *in vivo* location of amyloid plaques have also been shown [3, 4]. In *in vivo* PET studies, Alzheimer's disease (AD) patients have been shown to have a higher AV-45 retention than healthy controls (HC) [5, 6], even at early stages [7]. These characteristics point to AV-45 uptake, together with other amyloid ligands, as a good biomarker of amyloid pathology and Alzheimer's disease, and as a possible aid to clinical diagnosis. Anyway, in the clinical practice, visual analysis is the most used exploitation method for AV-45 images. Although useful in clinical practice, visual analysis could lead to limited sensitivity and specificity [8].

Most studies have so far focused on voxel-wise analyses [9] and global AV-45 uptake [6]. However, AV-45 has also shown non-specific binding in white matter [6]. White matter is a tissue mainly composed of myelin, which is highly lipidic. The lipophilic affinity of AV-45 [1, 9] may thus explain the non-specific binding in this tissue [8]. Consequently, both healthy subjects and AD patients show important binding of AV-45 in white matter [6]. Furthermore, the lack of specific binding should lead to comparable uptake of AV-45 in the white matter of healthy subjects and AD patients. Trying to avoid this issue, recent studies have used different methods in order to focus on AV-45 uptake in the grey matter, excluding white matter from the analysis [7, 10, 11]. Only a few previous studies have investigated differential binding of amyloid biomarkers in white matter tissue. Authors failed to find any difference between AD and HC white matter's uptake, either using the fluoride amyloid marker florbetaben or the carbonate amyloid marker PiB [12-14]. To our knowledge, no study regarding the differential binding of AV-45 amyloid marker in white matter between AD patients and healthy controls have been led so far. Moreover, little is known about the differential AV-45 uptake observed between grey and white matters for each group.

The aim of this study was (i) to determine and compare the pattern of AV-45 binding in white matter in AD and HC, (ii) to compare the binding patterns in white and grey matters within each group and (iii) to investigate if more subtle uptake quantification can lead to better discrimination performance. For this purpose, we investigated AV-45 uptake in patients presenting with AD at early stage and matched, healthy subjects. In order to characterize AV-45 uptake in white and grey matters, we used an approach based on counts per second histograms.

2. Materials and Methods

2.1 Subjects

All participants gave their written informed consent. This study was approved by the local ethics committee (Comité de Protection des Personnes Sud-Ouest et Outre-Mer I) and the French Agency for Safety and Security of Medical Devices (Agence Française de Sécurité Sanitaire des Produits de Santé, reference A90605-58).

Patients at the prodromal stage of Alzheimer's disease (AD) over 65 years old and matched healthy controls (HC) were recruited. All patients came from the outpatient memory clinic (Neurology department, University Hospital, Toulouse, France), and presented with a memory complaint dating from more than six months. They were selected according to research criteria for prodromal Alzheimer's disease [15]: they had to show isolate memory impairment on neuropsychological assessment and one or more of the following features:

- medial temporal lobe atrophy assessed on MRI scan (sequences detailed below);
- temporo-parietal hypometabolism pattern on cerebral fluorodesoxyglucose (FDG)-PET scan ;
- abnormal CSF biomarkers according to published criteria [16]

Patients were not included if they had a concomitant neurologic or psychiatric disease history, or if they had any clinically significant pathology that could explain the memory complaint. Significant white matter hyperintensities found on T2 MRI scan were motive of exclusion.

Healthy controls were recruited among patients' relatives or using recruitment posting in public places. They were not included if they had any neurologic or psychiatric disease history, or if they had first-degree relatives with Alzheimer's disease. They underwent the same neuropsychological assessment and same imaging exams (MRI, FDG-PET) as patients. They had no memory complaint, and showed neither cognitive impairment on the neuropsychological assessment nor abnormalities on MRI scan.

All participants included underwent a second PET-scan using florbetapir (AV-45) amyloid marker (details on acquisition below).

All these examinations were spread over three different appointments, scheduled within 3 months maximum. More details on the population recruitment is available elsewhere [7].

2.2 Images Acquisition

A brain MRI scan was performed in all participants using a Philips 3-T imager (Intera Achieva, Philips, Best, The Netherlands). A high resolution anatomical image, using a 3D-T1 weighted sequence (in-plane resolution 1 x 1mm, slice thickness 1mm, repetition time/echo time/inversion time = 8,189 ms/3.75 ms/1012.2 ms, flip angle 8°, field of view 240 x 256, and 160 contiguous slices) and a T2-weighted sequence (reconstructed resolution 0.45x0.45x3 mm^3, repetition time/echo time = 4 132 ms/80 ms ms, flip angle 90°, field of view 240 x 184, and 43 slices) were achieved.

AV-45 PET combined with a CT scans were performed on a hybrid PET/CT Biograph 6 TruePoint HiRez (Siemens medical Solutions). This PET/CT operated in 3D detection mode. The images were reconstructed using 3D ordered subset expectation maximization

(OSEM) algorithm (4 iterations, 16 subsets) with corrections for random, scatter, and attenuation provided by the manufacturer. Partial volume effect correction was performed using the Point Spread Function (PSF) modelisation implemented by Siemens (HD-PET©). The acquisitions were performed 50 minutes after intravenous administration of 3.4±0.4 MBq/kg of ^{18}F Florbetapir for twenty minutes list mode acquisitions.

2.3 Visual Analysis

AV-45 PET scan images were visually assessed by three observers (two Nuclear Medicine physicians and one Radiologist physicist) who received a special training program, blind to clinical diagnosis. Images were quoted as amyloid-positive or negative by comparing the cortical grey and white matter AV-45 uptakes. Following the recommendations given by AV-45 producer (Lily®), a scan was rated as positive when contrast between grey and white matter was lost in two or more brain areas (each area being larger than a single cortical gyrus) or when the scan showed one or more areas (each area being larger than a single cortical gyrus) in which gray matter's radioactivity was intense and clearly exceeded radioactivity of adjacent white matter (http://pi.lilly.com/us/amyvid-uspi.pdf). Finally, amyloid profile was considered positive when at least two observers rated the scan as positive, otherwise it was considered negative. The discriminant power of AV-45 imaging visual rating was calculated using specificity (percentage of healthy controls rated amyloid negative) and sensitivity (percentage of AD patients rated amyloid positive). Fleiss' kappa was calculated as measure of agreement [17].

2.4 Image Analysis

Segmentation of grey and white matter was achieved using SIENAX and FIRST (FSL library's tools) from the 3D-T1 MRI image of each participant. AV-45 images were registered

onto the subjects' anatomical space defined by the T1 images. In order to do so, CT scans of each subject were first linearly registered to the relative T1 image. The transformation matrix obtained from this linear registration was then applied to the AV-45 images, so that AV-45 images were coregistered in the T1 space. For subsequent analysis, only data pertaining to grey and white matter were used (Figure 1).

2.5 Standard Uptake Value calculation

In order to assess mean uptake, the mean count per voxel was extracted for all segmented AV-45 images for the grey and white matter, separately. The whole grey and white matter maps were taken into account for this quantification. These values were then divided by the mean count per voxel of the whole cerebellum (vermis excluded), in order to obtain standard uptake value ratio [3, 6][3, 9].

Mean SUVr of white matter between AD and HC groups were compared using two sample t-tests. This comparison was also achieved for grey matter. SUVr for grey and white matter were compared within each group using a Wilcoxon test.

2.6 Histogram

2.6.1 Histogram definition

Using FSL software, we created for each subject an AV-45-intensity (counts per second) histogram for grey and white matters. The intensity range of each image was divided into 200 bins and the frequency of occurrence of each intensity value (i.e. the number of voxels falling in that intensity range) was computed for each bin (see figure 1). In order to allow a direct comparison between histograms, we divided the frequency of occurrence of each intensity bin by the total number of voxels in the tissue analyzed.

To assess the possible effect the threshold chosen for the grey and white matter mask may have on the intensity histograms, we randomly chose one HC and one AD patient and we created grey and white matter masks using a probability gradient : thresholds at .25, .50, .75 and .95., corresponding to a probability of respectively 25%, 50%, 75% and 95% of being grey/white matter. A histogram for each one of the mask was then created (i.e. 8 histograms per subject, 4 for grey matter and 4 for white matter). These histograms were then plotted to visually inspect for differences related to the chosen thresholds (supplementary Figure 1).

Finally, to rule out the possible effect of AV-45 signal spill out from grey matter to white matter, we calculated a conservative white matter mask. AV-45 white matter images were eroded using a Gaussian kernel of 1mm isotropic in order to exclude white matter voxels confining with grey matter voxels. Histograms were derived from these eroded images.

In a further effort to control for possible confounds in the white matter, we automatically segmented white matter hyperintensities for both AD and HC subjects and masked the white matter AV-45 images for these hyperintensities (see supplementary data for methodological details).

--Insert Figure 1 about here--

2.6.2 Histogram Analysis

Different indexes were extracted from the histograms of each subject in grey and white matters separately. We calculated the 10^{th} and the 90^{th} percentiles of occurrence frequency, the median bin, the kurtosis, the skweness, the maximal bin, the area under the curve below the maximal bin (ABM), the maximal frequency and the histogram width. These indexes are among the most commonly used in histogram analyses [18-20].

To assess the relationship between white and grey matters within each subject, we calculated the euclidean distance between white and grey matter histograms' peaks. The difference between Euclidean distances in the two groups was assessed by a two sample t-test.

Given the non-Gaussian distribution of the different indexes, data were first transformed in ranks in order to achieve parametric statistical test [21]. The obtained ranked histogram indexes were then submitted to 4 different MANOVAs: 2 MANOVAs assessing differences between the two groups, and two MANOVAs assessing differences between white and grey matter within each group. The effect size of the analyses was calculated using the partial eta-squared, that represents the ratio between the variance explained by the factor of interest and the sum of the total variance and the variance of the error. The partial eta-squared represents, in this context, the proportion of variance explained by the group factor. The multivariate analyses were performed using both the histograms extracted from the original AV-45 white matter images, the ones extracted from eroded white matter images, in order to control for spill out effect. A supplementary multivariate analysis was performed on histogram parameters extracted from AV-45 white matter images masked for hyperintensities.

For both grey and white matter, the difference between groups for each index was tested using canonical univariate analysis.

2.7 Classification

2.7.1 Discriminant Analysis

In order to assess whether histogram analysis may improve the ability of classical quantitative SUVr assessment to discriminate AD patients from HC participants [8, 22], three different discriminant analyses were performed: an analysis using individual mean SUVr only; a second analysis combining all the histogram indexes; a third analysis combining the two previous ones. These analyses were performed on white and grey matters separately and

then both taken together. These analyses, performed on Matlab (Statistic Toolbox), were submitted to a leave one out cross-validation.

For each discriminant analysis the specificity and sensitivity have been calculated. Specificity was defined as the percentage of healthy controls correctly classified (i.e. the percentage of true negative). The sensitivity was defined as the percentage of AD patients correctly classified (i.e. the percentage of true positive).

2.7.2 Histogram-based cluster analysis

In order to obtain a data driven classification of the subjects on the basis of their histograms -without feeding the model with diagnostic label - the white and grey matters' histograms indexes were submitted to a cluster analysis performed in Matlab environment. This analysis was based on a k mean clustering repeated 20 times, maximizing the cosine distance between clusters centroids. Three models with 2, 3 and 4 clusters were implemented and the model with the best fitting (calculated as the mean of the silhouette values) was retained.

3. Results

3.1 Population

24 prodromal AD patients and 17 healthy controls matched in age, gender, level of education were recruited. Table 1 reports demographic and neuropsychological data.

-Insert Table 1 here –

3.2 Visual Analysis

3 out of 24 AD patients were classified as AV-45 negative and 2 out of 17 HC subjects were classified as AV-45 positive. The visual assessments lead to a specificity of 88.2% and a sensitivity of 87.5% (see table 2). The Fleiss' kappa was equal to 0.80, indicating substantial agreement between raters.

3.3 SUVr comparisons

3.3.1 White and grey matters between groups

In the white matter, there was no significant difference regarding mean SUVr between the two groups (mean for HC=1.92 ± 0.23; mean for AD patients = 1.97 ± 0.3, p=.585). Mean SUVr of grey matter was significantly higher for AD patients (1.56 ± 0.3) than for HC participants (1.22 ± 0.1, t=4.36, p<.001).

3.3.2 White versus grey matter within group

Mean intensity value was significantly higher in white matter compared to grey matter in both groups (t=-15.98 for HC participants, t=-13.06 for AD patients, p<.001 for both groups).

3.4 Histogram Comparisons

3.4.1 Comparison of white and grey matters histograms between groups

AD grey and white matter histograms seem, as a whole, to have greater area in the right half of the graph, meaning a higher frequency of high-intensity voxels relative to HC (Figure 2 a-b). Visually, white and grey matters histograms were closer for AD patients relative to healthy controls. The euclidean distance between the grey and white matter histograms' peaks was higher in the HC group (mean=63.74 ± 17.30) compared to the AD group (mean=37.19 ± 16.61, t=-4.99, p<.0001). The same analysis performed using the histograms obtained from the eroded AV-45 white matter images lead to comparable results (see Supplementary Table 1).

--Insert Figure 2 about here—

3.4.2 Comparison of white and grey matters histograms within each group

The shape of white and grey matter histograms was different for both HC and AD groups. This is confirmed by significant differences on multivariate analysis (Lambda =.4, p<.05; for AD and Lambda =.09, p<0005 for HC).

As for the multivariate analyses, both white (Lambda=5.2, p<.001, partial eta-squared= 0.51) and grey (Lambda=5.9, p<.001, partial eta-squared= 0.59) matter histograms differed between AD and HC subjects. The MANOVA performed on white matter histogram parameters remained significant when white matter images masked for hyperintensities were used (see supplementary data). Regarding the white matter histograms, only kurtosis, skweness and maximum frequency significantly diverged in the two samples. While kurtosis, skweness and maximum frequency were higher in the AD groups, the histogram width was higher for HC subjects (Figure 2). As for the grey matter histograms, the univariate analyses performed on each index revealed that all the indexes were significantly different between the

two groups. Median, maximal bins, and ABM were higher for AD groups, while the 4 other indexes were higher for the HC group (Figure 2). Figure 3 reports in spider-web graphs the mean indexes for grey and white matter in the two groups. The same analysis performed using the histograms obtained from the eroded AV-45 white matter images lead to comparable results (see Supplementary Table 1).

3.4.3 Probability Gradient

Histograms derived from the different thresholds elected did not show important changes on visual assessment, confirming the validity of grey and white matter segmentation (see supplementary Figure 1).

--Insert Figure 3 about here—

3.5 Classification

3.5.1 Discriminant analyses

Discriminant analyses on either SUVr values, histograms indexes only, or both SUVr and histogram indexes, always showed higher specificity and sensitivity for grey matter only. Discriminant analysis using SUVr values led to better specificity and sensitivity when taking into account grey matter only (82.4% and 79.2%, respectively), compared to white matter only (35.3% and 54.2%, respectively) or both grey and white matter (29.4% and 95.8% respectively).

Similarly, discriminant analyses on histograms parameters only, specificity and sensitivity were higher taking into account grey matter only (88.2% and 91.7%, respectively), compared to white matter only (58.8% and 87.5%, respectively) or both grey and white matter (76.5% and 83.3% respectively).

Discriminant analyses using both histograms parameters and SUVr showed better specificity and sensitivity with grey matter only (82.3% and 87.5%, respectively), compared to white matter only (58.8% and 83.3%, respectively) or both grey and white matter (76.5% and 83.3% respectively).

Overall, the best trade-off between specificity and sensitivity (the smallest proportion of misclassified patients associated with the smallest proportion of misclassified HC subjects) was reached using grey matter histogram indexes *without* the SUVr (Table 2).

Of note, when the analysis relied on grey and white matters together, adding the mean SUVr to histograms indexes did not improve the classification performance.

--Insert Table 2 about here --

The histograms of misclassified subjects were plotted with AD and HC mean histograms (Figure 4). For grey matter based classification (Figure 4.a) the two misclassified healthy controls have part of the histogram beyond the 75^{th} percentile of the AD grey matter mean histogram. As for the 2 misclassified AD, their histograms have both higher peak and narrow curves relative to AD mean histogram.

Regarding histograms of the white matter only, we selected 4 misclassified subjects (2 AD and 2 HC) for easier reading of the figure (Figure 4.b), as profiles were very heterogeneous (see supplementary figure 2). Two of them, one AD and one HC, showed right-shifted histograms with peaks below the 25^{th} percentiles of their respective groups' mean histograms. The two others showed histogram' shapes similar to their respective groups'.

--Insert Figure 4 about here—

3.5.2 Cluster Analysis

The cluster analysis performed on the grey and white matter histograms indexes revealed that the best model (i.e. the solution with the lowest mean silhouette value) was based on two clusters. Cluster 1 comprehends 3 AD patients and 15 HC, while cluster 2 comprehends 21 AD patients and 2 HC. Cluster 1 and cluster 2 mean histograms shapes are similar to the ones of HC and AD respectively (Figure 2). However, some shapes differences can be observed between Cluster 1 and HC mean histogram, and between Cluster 2 and AD mean histogram, in particular for the white matter. It is noteworthy that the subjects which were misclassified in the discriminant analyses do not belong to the same cluster.

4. Discussion

The aim of this study was to compare patterns of AV-45 uptake in white matter of Alzheimer's disease patients and healthy controls and to compare AV-45 uptake in white and grey matter within this two groups.

As expected, we showed that AV-45 uptake in grey matter was higher in AD patients compared to HC using SUVr analysis. However, white matter uptake was higher than grey matter's uptake in both groups, using the same method. Despite the lack of difference found between the two groups in white matter using SUVr, our innovative AV-45 uptake assessment using histograms showed differences between the two groups within this tissue. Such difference in AD's and HC's white matter histograms was present also when the comparison involved the histograms derived from the eroded AV-45 white matter images. This suggests such difference cannot be attributed to a spill out of the AV-45 signal from the grey to the white matter. However, inclusion of white matter in the discriminant analysis did not improve the classification performance but the histogram indexes outperformed SUVr in such classification. To our knowledge, no other study has investigated differential AV-45 uptake in white and grey matter of AD patients and healthy controls.

Regarding grey matter, the mean SUVr was higher for AD patients than for healthy controls. These results confirm that amyloid deposition in the AD patients grey matter, as measured by AV-45 SUVr, is significantly higher relatively to healthy controls [4, 6]. Recent work using MRI based segmentation methods have shown similar results in prodromal AD patients [7] The histogram analysis also showed significant difference between the two groups on every single index used.

In white matter, mean SUVr was higher than in grey matter for both groups. This result confirms the high lipophilic nature of AV-45 [1, 8, 9]. No difference was found on SUVr analyses between prodromal AD patients and healthy controls groups, in line with previous reports using different amyloid markers like PiB [13, 14] and florbetaben [12, 13]. Interestingly, histogram analyses did reveal significant differences in this tissue as patients with AD showed greater width, kurtosis, skweness and maximal frequency than healthy controls. This difference suggests that not all uptake in white matter is non specific. This kind of results has never been shown using AV-45 PET imaging. However, using other imaging modalities such as MRI, white matter modifications (e.g. axonal injury and white matter tract degradation) in AD patients have recently been discovered [23-25]. In their study, Zhang and colleagues showed a reduction of fractional anisotropy (FA) using DTI sequences in a group of AD patients, while Canu and colleagues (2011) found increased mean diffusivity (MD) in AD patients in several cortical tracts. Such results are consistent with white matter tracts degradation. These modifications may be related to the differences observed in our study between the AD and the HC white matter and further work is needed to determine the cause of the differences we report. Apart from white matter microstructural changes revealed by DTI imaging, the difference we observed between AD's and HC white matter histograms may be related to white matter hyperintensities (WMHs). WMHs volume have been shown to be associated to cognitive performance in AD patients more than in MCI and HC [26].Moreover

WMHs are more hypoperfused in AD patients then in HC [27]. However, to our knowledge, there are no study focusing on the relationship between AV-45 uptake in the white matter and WMHs, although a study performed using PiB showed that amyloid burden is correlated to index of microstructural damage in WMHs[28]. We showed that, in our study, WMHs did not seem to explain the observed difference (see supplementary data). Future investigations, including FLAIR imaging, are necessary to spread light on this topic. Independently from the pathophysiological causes of histograms difference, the intensity histogram analysis may be able to reveal pathological changes in the AD white matter that are shadowed by non specific binding when only mean SUVr is taken into account. As a remark, it is noteworthy that grey and white matter histograms look alike in the AD sample, and that euclidean distance between grey matter and white matter peaks is diminished compared to healthy controls. Moreover, in figure 3, AD grey matter's plots looked like to HC white matter's plots. This may suggest similar properties of the grey matter tissue in AD and the white matter tissue in HC. Further investigations using multimodal PET amyloid and MRI imaging in the same sample are required to understand this phenomenon. Observing differential AV-45 white matter uptake in a pathological population compared to healthy subjects speaks in favour of the possibility of using such marker to study diseases related to white matter disorders. Indeed some studies yet used PiB to study white matter status in different pathologies or neurological conditions. In particular PiB was used to investigate white matter modifications after traumatic brain injury [29] and in leukoaraiosis [28, 30]. The latter studies found that PiB uptake in the white matter was correlated to WMHs volume in cerebral amyloid angiopathy patients but not in AD [30], and that PiB positivity in the white matter was associated to reduction of the fractional anisotropy [28]. To our knowledge, AV-45 has not yet been used for investigating white matter pathologies.

Despite the significant difference in white matter AV-45 uptake between AD and HC enlightened by histogram analysis in our study, discriminant analyses suggest that white matter is not useful to classify AD and HC subjects. While discriminant analyses based on grey matter histogram indexes only lead to highest specificity and sensitivity, white matter based classification showed a high sensitivity but dramatically poor specificity. When indexes of both grey and white matter histogram were used, the performance of the discriminant model was worse, suggesting that white matter brings noise in the classification. A few studies on amyloid markers have also reported good classification performance using different methods. A recent study using the amyloid marker flutemetamol showed a specificity and sensitivity of 92% and 85.2%, respectively, to discriminate patients with mild cognitive impairment (MCI) from HC, using a learning machine method [25]. Discriminant analyses in AD have also been widely used in other modalities such as MRI [31], or combinations of modalities [32, 33]. In their classification study based on combined features of structural MRI sequences, Wolz et al. reported a specificity of 85% and sensitivity of 93% for discrimination between AD and HC, but only a specificity of 82% and sensitivity of 86% between patients with MCI and HC [34].Of note, white matter histograms in our analysis showed a great variability (figure 4), which could be the reason why white matter indexes do not improve the classification.

Several white matter modifications related to aging have been described in the MRI literature [35-37]. Moreover, it has been shown that vascular amyloid deposit increases with age, which may lead to significant AV-45 uptake. Taken together these age-related modifications may partly explain the observed variability in white matter histogram profiles. These hypotheses would require more investigations, targeting directly these issues.

The evidence from the discriminant analysis should be read together with the results of the cluster analysis, in which the classification was performed without the a priori label of the

diagnosis. The best solution was a model with two clusters, confirming that two general white and grey histogram intensity profiles were present in the two samples. These two clusters roughly correspond to the two diagnostic samples of the study. We propose that the two clusters would correspond to “AV-45 binder” and “AV-45 non binder”. Indeed, the leftward peak of cluster 1 grey matter mean histogram clearly represents low fixation (non binder, Figure 2-a) while histogram shape for cluster 2 suggests high uptake values (binder, Figure 2-b). Moreover, a total non specific binding in the white matter should lead to a comparable (high) AV-45 fixation in the two groups. The presences of significant difference in white matter histogram suggest that some form of specific binding exists in the white matter.

As a final note, the finding that 4 AD patients were amyloid negative and 2 healthy controls were amyloid positive on visual assessment is in line with the findings in the literature [9][6]. More interesting is the convergence between visual rating and cluster analysis, two methods without any a priori. Comparing the members of the two clusters and the visual assessment results, we found that the two HC members of the cluster number 2, which contains mainly AD patients, are the same HC rated as amyloid-positive on visual analysis. In the same way, the 3 AD patients classified in the cluster number 1, which contains mainly HC, were rated as amyloid-negative on visual assessment. Compared to these two without a priori methods, the analysis with a priori (i.e. discriminant analysis) showed slightly better classification performances. This suggests that one should favor discriminant model based on clinical information rather than unsupervised model.

5. Conclusion

In this study, we first demonstrated differential AV-45 binding in white matter between patients with Alzheimer's disease at an early stage and healthy controls. White matter binding is thus not exclusively non specific as sometimes proposed. This information is not detectable using mean SUVr approach, but becomes clear when histogram indexes analyses are performed. Our results suggest that white matter AV-45 uptake, although not useful in discriminating between AD patients and HC, may carry information on white matter integrity and help study white matter in these populations. We also showed that the use of grey matter histogram indexes reaches the best sensitivity and specificity for AD and HC discrimination. Such results demonstrate that histogram approach could be useful in clinical practice.

Acknowledgements: This study was supported by a grant from the University Hospital of Toulouse, local grant 2007, and a grant from the Agence Nationale de la Recherche. The authors thank the promoter of this study and CHU Toulouse.

Conflict of Interest: The authors declare that they have no conflict of interest.

References

1. Choi, S.R., et al., *Preclinical properties of 18F-AV-45: a PET agent for Abeta plaques in the brain.* J Nucl Med, 2009. **50**(11): p. 1887-94.
2. Carpenter, A.P., Jr., et al., *The use of the exploratory IND in the evaluation and development of 18F-PET radiopharmaceuticals for amyloid imaging in the brain: a review of one company's experience.* Q J Nucl Med Mol Imaging, 2009. **53**(4): p. 387-93.
3. Clark, C.M., et al., *Cerebral PET with florbetapir compared with neuropathology at autopsy for detection of neuritic amyloid-beta plaques: a prospective cohort study.* Lancet Neurol, 2012. **11**(8): p. 669-78.
4. Clark, C.M., et al., *Use of florbetapir-PET for imaging beta-amyloid pathology.* JAMA, 2011. **305**(3): p. 275-83.
5. Lin, K.J., et al., *Whole-body biodistribution and brain PET imaging with [18F]AV-45, a novel amyloid imaging agent--a pilot study.* Nucl Med Biol, 2010. **37**(4): p. 497-508.
6. Wong, D.F., et al., *In vivo imaging of amyloid deposition in Alzheimer disease using the radioligand 18F-AV-45 (florbetapir [corrected] F 18).* J Nucl Med, 2010. **51**(6): p. 913-20.
7. Saint-Aubert, L., et al., *Cortical florbetapir-PET amyloid load in prodromal Alzheimer's disease patients.* Eur J Nucl Med Mol Imaging, 2013. **3**(1).
8. Camus, V., et al., *Using PET with 18F-AV-45 (florbetapir) to quantify brain amyloid load in a clinical environment.* Eur J Nucl Med Mol Imaging, 2012. **39**(4): p. 621-31.
9. Fleisher, A.S., et al., *Using positron emission tomography and florbetapir F18 to image cortical amyloid in patients with mild cognitive impairment or dementia due to Alzheimer disease.* Arch Neurol, 2011. **68**(11): p. 1404-11.
10. La Joie, R., et al., *Region-specific hierarchy between atrophy, hypometabolism, and beta-amyloid (Abeta) load in Alzheimer's disease dementia.* J Neurosci, 2012. **32**(46): p. 16265-73.
11. Rodrigue, K.M., et al., *beta-Amyloid burden in healthy aging: regional distribution and cognitive consequences.* Neurology, 2012. **78**(6): p. 387-95.
12. Villemagne, V.L., et al., *Amyloid imaging with (18)F-florbetaben in Alzheimer disease and other dementias.* J Nucl Med, 2011. **52**(8): p. 1210-7.
13. Villemagne, V.L., et al., *Comparison of 11C-PiB and 18F-florbetaben for Abeta imaging in ageing and Alzheimer's disease.* Eur J Nucl Med Mol Imaging, 2012. **39**(6): p. 983-9.
14. Fodero-Tavoletti, M.T., et al., *Characterization of PiB binding to white matter in Alzheimer disease and other dementias.* J Nucl Med, 2009. **50**(2): p. 198-204.
15. Dubois, B., et al., *Research criteria for the diagnosis of Alzheimer's disease: revising the NINCDS-ADRDA criteria.* Lancet Neurol, 2007. **6**(8): p. 734-46.
16. Wallon, D., et al., *The French Series of Autosomal Dominant Early Onset Alzheimer's Disease Cases: Mutation Spectrum and Cerebrospinal Fluid Biomarkers.* Journal of Alzheimers Disease, 2012. **30**(4): p. 847-856.
17. Fleiss, J.L., J.C.M. Nee, and J.R. Landis, *Large Sample Variance of Kappa in the Case of Different Sets of Raters.* Psychological Bulletin, 1979. **86**(5): p. 974-977.
18. Kyriazi, S., et al., *Metastatic ovarian and primary peritoneal cancer: assessing chemotherapy response with diffusion-weighted MR imaging--value of histogram analysis of apparent diffusion coefficients.* Radiology, 2011. **261**(1): p. 182-92.
19. Pope, W.B., et al., *Recurrent glioblastoma multiforme: ADC histogram analysis predicts response to bevacizumab treatment.* Radiology, 2009. **252**(1): p. 182-9.
20. Pope, W.B., et al., *Apparent diffusion coefficient histogram analysis stratifies progression-free survival in newly diagnosed bevacizumab-treated glioblastoma.* AJNR Am J Neuroradiol, 2011. **32**(5): p. 882-9.
21. Conover, W.J. and R.L. Iman, *Rank Transformations as a Bridge between Parametric and Nonparametric Statistics - Rejoinder.* American Statistician, 1981. **35**(3): p. 132-133.

22. Barthel, H., et al., *Cerebral amyloid-beta PET with florbetaben (18F) in patients with Alzheimer's disease and healthy controls: a multicentre phase 2 diagnostic study.* Lancet Neurol, 2011. **10**(5): p. 424-35.
23. Canu, E., et al., *Mapping the structural brain changes in Alzheimer's disease: the independent contribution of two imaging modalities.* J Alzheimers Dis, 2011. **26 Suppl 3**: p. 263-74.
24. Firbank, M.J., et al., *Diffusion tensor imaging in Alzheimer's disease and dementia with Lewy bodies.* Psychiatry Res, 2011. **194**(2): p. 176-83.
25. Vandenberghe, R., et al., *Binary classification of ^{18}F-flutemetamol PET using machine learning: comparison with visual reads and structural MRI.* Neuroimage, 2013. **64**: p. 517-525.
26. Kim, J.H., et al., *Regional white matter hyperintensities in normal aging, single domain amnestic mild cognitive impairment, and mild Alzheimer's disease.* J Clin Neurosci, 2011. **18**(8): p. 1101-6.
27. Makedonov, I., S.E. Black, and B.J. MacIntosh, *Cerebral small vessel disease in aging and Alzheimer's disease: a comparative study using MRI and SPECT.* Eur J Neurol, 2013. **20**(2): p. 243-50.
28. Chao, L.L., et al., *Associations between white matter hyperintensities and beta amyloid on integrity of projection, association, and limbic fiber tracts measured with diffusion tensor MRI.* PLoS One, 2013. **8**(6): p. e65175.
29. Hong, Y.T., et al., *Amyloid Imaging With Carbon 11-Labeled Pittsburgh Compound B for Traumatic Brain Injury.* JAMA Neurol, 2013.
30. Gurol, M.E., et al., *Cerebral amyloid angiopathy burden associated with leukoaraiosis: A positron emission tomography/magnetic resonance imaging study.* Ann Neurol, 2012.
31. Casanova, R.H., F.C.; Espeland, M.A.; Alzheimer's Disease Neuroimaging Initiative., *Classification of structural MRI images in Alzheimer's disease from the perspective of ill-posed problems.* PLoS One, 2012. **7**(10): p. e44877.
32. Jagust, W., et al., *What does fluorodeoxyglucose PET imaging add to a clinical diagnosis of dementia?* Neurology, 2007. **69**(9): p. 871-877.
33. Westman, E., J.S. Muehlboeck, and A. Simmons, *Combining MRI and CSF measures for classification of Alzheimer's disease and prediction of mild cognitive impairment conversion.* Neuroimage, 2012. **62**(1): p. 229-238.
34. Wolz, R., et al., *Multi-method analysis of MRI images in early diagnostics of Alzheimer's disease.* PLoS One, 2011. **6**(10): p. e25446.
35. Jeon, T., et al., *Regional changes of cortical mean diffusivities with aging after correction of partial volume effects.* Neuroimage, 2012. **62**(3): p. 1705-16.
36. Stadlbauer, A., et al., *Magnetic resonance fiber density mapping of age-related white matter changes.* Eur J Radiol, 2012. **81**(12): p. 4005-12.
37. Watanabe, H., et al., *Progression and prognosis in multiple system atrophy: an analysis of 230 Japanese patients.* Brain, 2002. **125**(Pt 5): p. 1070-83.

Figures

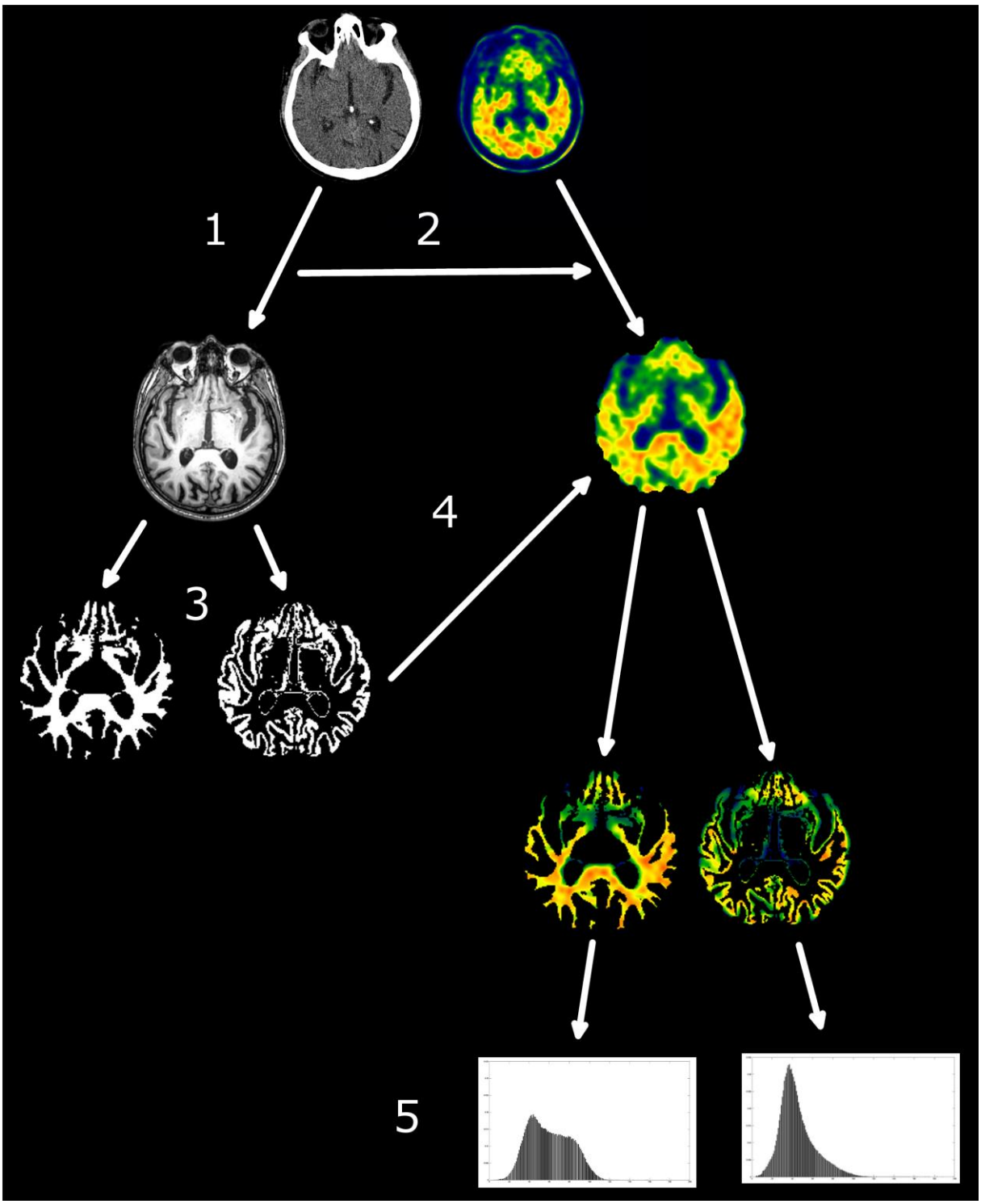

Figure 1: Pipeline for histogram creation. CT scan was registered on the T1 scan (1) and the transformation matrix applied to the PET AV-45 scan (2). T1 was segmented in grey and

white matter (3) and the binary masks of the tissues were applied to the PET AV-45 scan in T1 space (4). Intensity histograms were extracted from the tissues (5).

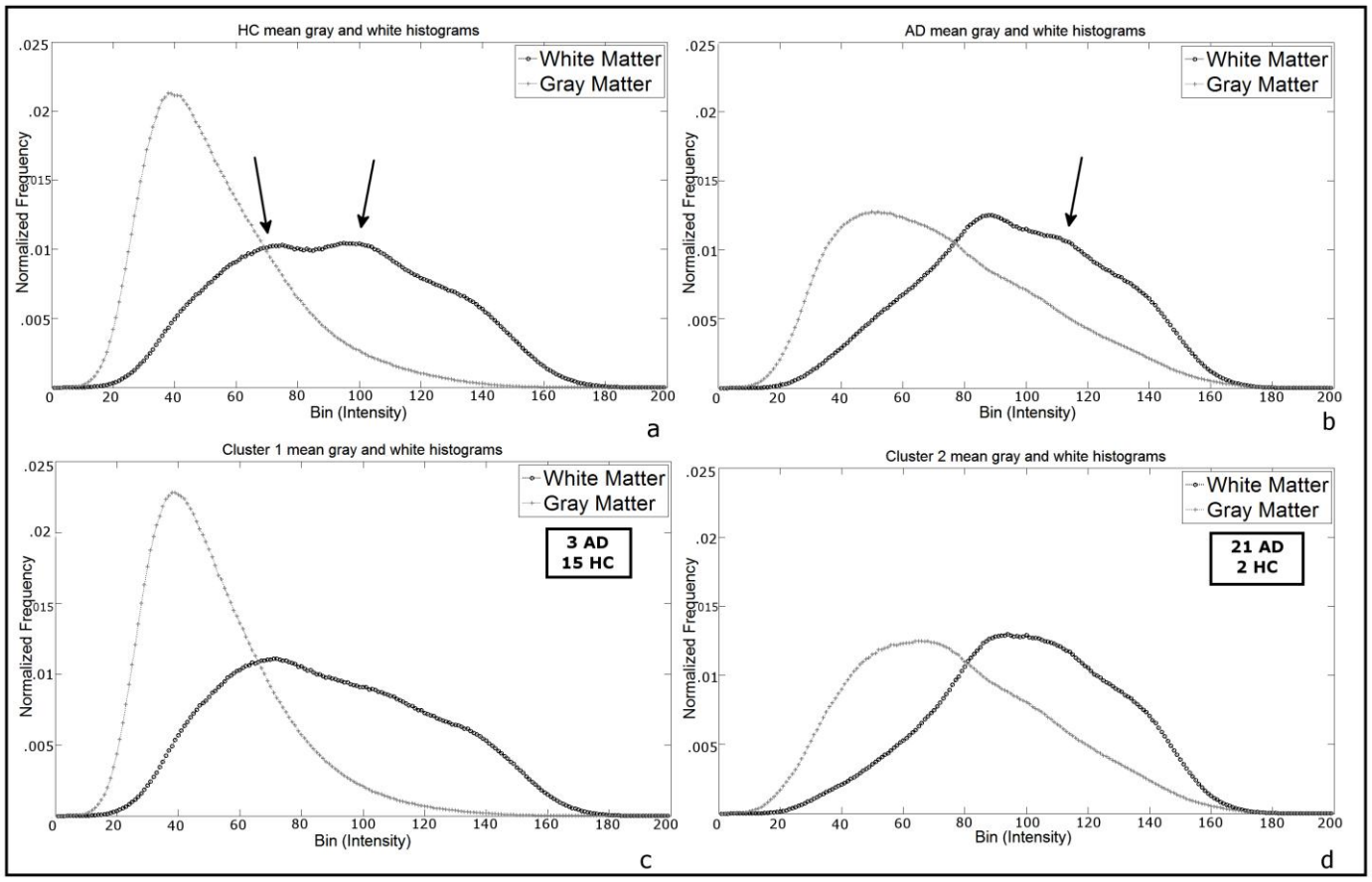

Figure 2.Mean histograms shapes. Upper row: grey and white matter mean histograms for (a) HC and (b) AD groups. Lower row: grey and white matter mean histograms for (c) subjects classified in cluster 1 and (d) subjects classified in cluster 2 (cf. the Cluster Analysis section). Arrows in (a) show shape difference relative to (c); arrow in (b) shows shape difference relative to (d), see Cluster Analysis below.

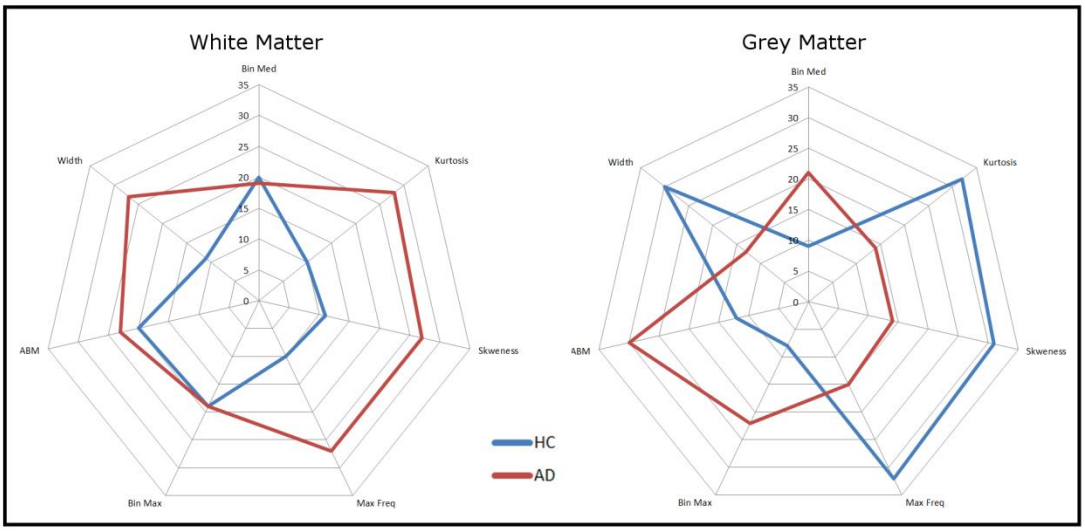

		HC	*AD patients*	*F test*	*p*
Grey Matter					
	Bin Med	8.53 (±2.60)	20.74 (±4.86)	14.24	<.001*
	Kurtosis	31.73 (±3.44)	15.00 (±5.65)	22.30	<.001*
	Skweness	31.53 (±3.60)	15.17 (±5.74)	20.09	<.001*
	Max Freq	31.27 (±3.94)	15.43 (±5.72)	17.73	<.001*
	Bin Max	7.60 (±2.03)	21.57 (±4.56)	24.18	<.001*
	ABM	11.67 (±3.32)	28.70(±5.60)	27.50	<.001*
	Width	30.20 (±4.01)	16.04 (±6.20)	12.92	<.001*
White Matter					
	Bin Med	18.53 (±4.49)	19.40 (±4.66)	.34	.441
	Kurtosis	12.20 (±5.01)	28.09 (±4.91)	26.92	<.0001*
	Skweness	12.67(±5.41)	27.61(±5.10)	21.39	<.0001*
	Max Freq	12.93 (±5.80)	27.26 (±5.09)	17.01	<.0001*
	Bin Max	19.27(±5.06)	20.51 (±5.35)	.41	.530
	ABM	21.93(±6.66)	23.61(±5.46)	.17	.547
	Width	14.80 (±7.06)	25.96 (±4.93)	9.94	<.005*

Figure 3: Upper panel. Spider web plots of the 7 histogram indices for (HC) and AD patients. Blue line = HC, red line = AD. Lower panel. Comparison of the histogram indexes in grey matter and in white matter between AD patients and HC subjects groups. Mean and (standard deviation) are mentioned for each index. Threshold significance for p=.05. Significant p values are mentioned with an asterisk.

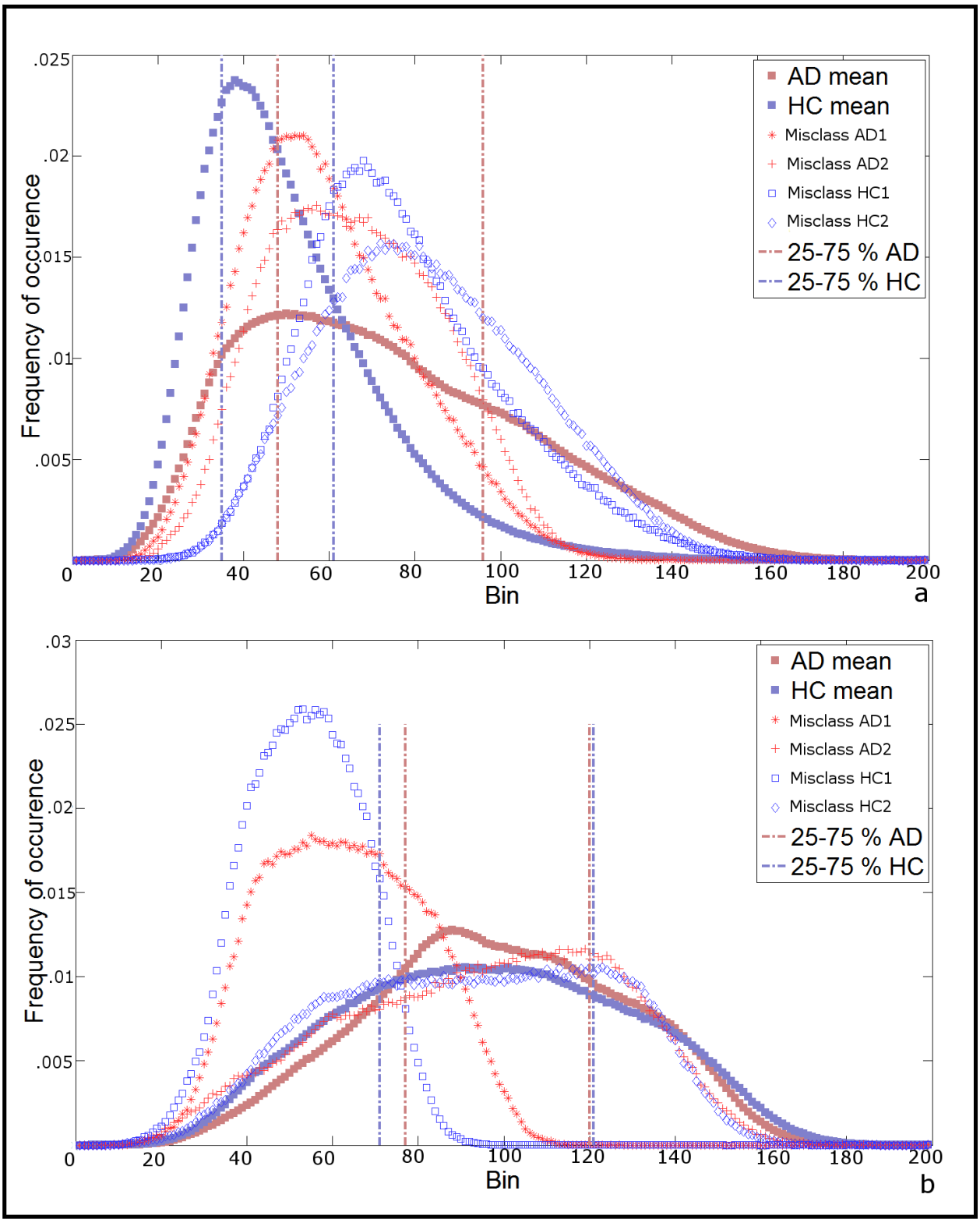

Figure 4. Histogram shape of misclassified subjects. a) Grey matter mean histograms of the 2 AD patients classified as HC (red stars and red crosses) and the 2 HC classified as AD (empty blue squares and diamonds) in the discriminant analysis performed on grey matter

histogram parameters plotted against the mean grey matter histogram of the correctly classified AD (filled red square) and HC (blue filled square). b) White matter mean histograms of 2 (out of 3) AD patients classified as HC (red stars and red crosses) and the 2 (out of 7) HC classified as AD (empty blue squares and diamonds) in the discriminant analysis performed on white matter histogram parameters, plotted against the mean white matter histogram of the correctly classified AD (filled red square) and HC (blue filled square). 1 out of 3 misclassified AD and 5 out of 7 misclassified HC are not shown for easiness of presentation, see supplementary Figure 2. Vertical pointed-dashed lines in both a and b panels mark 25^{th} and 75^{th} percentiles of histograms.

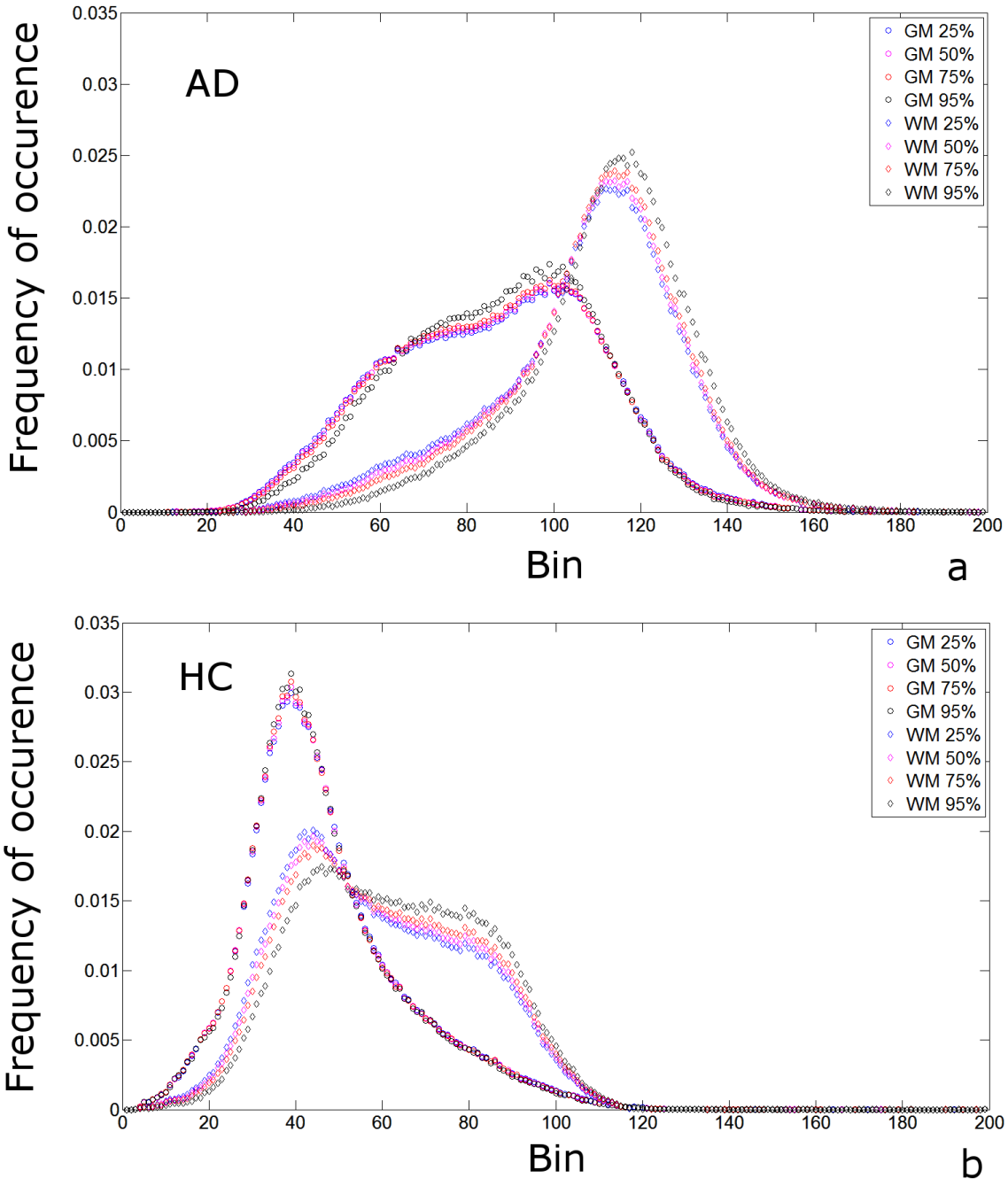

Supplementary Figure 1. *Intensity histograms of grey and white matter of an AD patients (a) and of a healthy control (b). Histograms were derived from grey and white matter probability images thresholded at 0.25, 0.50, 0.75 and 0.95, corresponding respectively to a probability of the 25%, 50%, 75% and 95% of a voxel of being in grey/white matter. No differences realted to the elected threshold are present.*

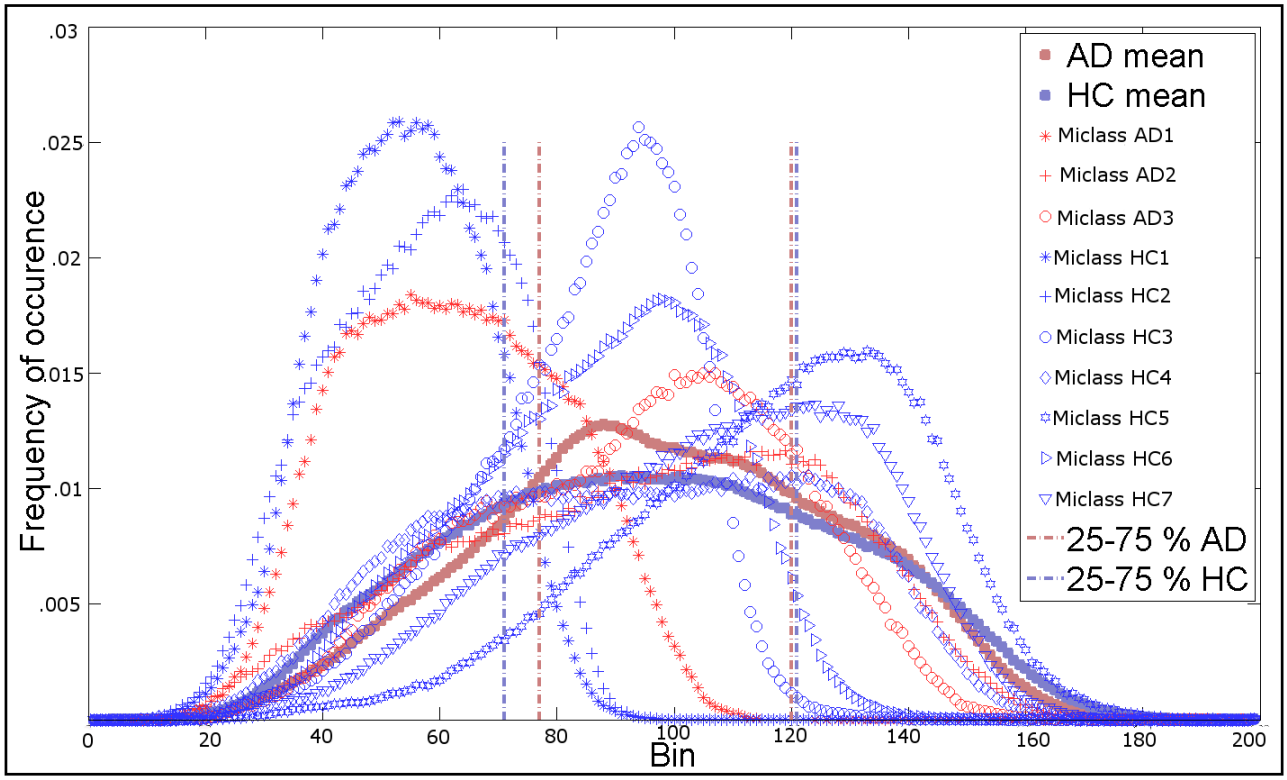

Supplementary Figure 2. *White matter mean histograms of AD (red filled squares) and HC (blue filled squares) and white matter histograms of the 3 AD patients and of the 7 HC subjects misclassified on the discriminant analysis performed using white matter indexes. The mean histograms were calculated without the misclassified subjects in each group. Vertical pointed-dashed lines in both a and b panels mark 25th and 75th percentiles of histograms.*

Tables

	AD patients	HC subjects	
Age	72.5(±4.9)	69.9(±4.8)	p= 0.077
Gender	12M / 12F	7M / 10F	χ^2= 0.491
Level of education (Years)	11.4(±2.7)	12.8(±3.3)	p= 0.193
CDR-scale score	0.6(±0.2)	.0(±.0)	p<.001
MMSE (/30)	24.9(±2.4)	28.4(±0.7)	p<0.001*

Table 1. Demographic and neuropsychological data for the Alzheimer patients (AD) and healthy controls (HC) group. M: Male; F: Female. CDR:Clinical Dementia Rating.

**: p<0.05.*

	Parameters	**Specificity**	**Sensitivity**	**FP**	**FN**
SUVr	Grey SUVr only	*82.4%*	*79.2%*	*3*	*5*
	White SUVr only	*35.3%*	*54.2%*	*11*	*7*
	Grey and White SUVr only	*29.4%*	*95.8%*	*12*	*1*
Histogram indexes	**Grey histogram only**	***88.2%***	***91.7%***	***2***	***2***
	White histogram only	*58.8%*	*87.5%*	*7*	*3*
	Grey and White histogram only	*76.5%*	*83.3%*	*4*	*4*
SUVr and histogram indexes	Grey All	*82.3%*	*87.5%*	*3*	*3*
	White All	*58.8%*	*83.3%*	*7*	*4*
	Grey and White All	*76.5%*	*83.3%*	*4*	*4*
Visual Rating		*88.2%*	*87.5%*	*2*	*3*

Table 2 . Specificity and sensitivity values for each discriminant analysis and for the visual rating of AV-45 PET scans . The discriminant analyses were performed using the SUVr only (SUVr only), the histogram indexes (histogram only), and both histograms indexes and SUVr (All). Specificity, sensitivity, number of false positive (FP) and false negative (FN) are mentioned for each analysis. False positive refers to healthy controls classified as AD in the discriminant analyses or in the visual rating. False negative refers to AD patients classified as healthy controls in the discriminant analyses or in the visual ratings. The analysis leading to the best trade-off between the two measures is in bold.

White Matter

Eroded

		HC	***AD patients***	***F test***	***p***
Univariate analysis on white matter histogram indexes	*Bin Med*	18.53 (±4.49)	19.40 (±4.66)	.77	.441
	Kurtosis	12.20 (±5.01)	28.09 (±4.91)	20.51	<.0001*
	Skweness	12.67(±5.41)	27.61(±5.10)	17.01	<.0001*
	Max Freq	12.93 (±5.80)	27.26 (±5.09)	16.66	<.0001*
	Bin Max	19.27(±5.06)	20.51 (±5.35)	.15	.696
	ABM	21.93(±6.66)	23.61(±5.46)	.773	.383
	Width	14.80 (±7.06)	25.96 (±4.93)	8.67	<.01*

		HC	***AD patients***	***T test***	***p***
Euclidean Distance		85.73 (±14.94)	55.56 (±21.57)	3.06	<.001*

Supplementary Table 1. Upper part: Comparison of the histogram indexes in white matter (eroded mask) between AD patients and HC subjects groups. Mean and (standard deviation) are mentioned for each index. Threshold significance for p=.05. Significant p values are mentioned with an asterisk. Lower part: Comparison between euclidean distance between grey and white matter for healthy controls and Alzheimer's disease patients.